Aberrations induced by side-projected laser guide stars in laser tomography adaptive optics systems

Marcos A. van Dam[1a], Rodolphe Conan[2], Antonin H. Bouchez[3], and Brady Espeland[2]

[1] Flat Wavefronts, P.O. Box 1060, Christchurch 8140, New Zealand
[2] Research School of Astronomy & Astrophysics, Australian National University, Cotter Rd., Weston, ACT 2611, Australia
[3] Giant Magellan Telescope Observatory Corporation, P.O. Box 90933, Pasadena, CA 91109, USA

Abstract. A laser tomography adaptive optics (LTAO) system is currently under design for the Giant Magellan Telescope (GMT). This system has six laser guide stars (LGSs) in a regular hexagon. For systems engineering reasons, it is preferable to project the LGSs from the side of the telescope. Experience with the Keck II adaptive optics system and analytical modeling have shown that side-launched LGSs result in aberrations, called LGS aberrations, with a lot of power at low-spatial frequencies. This is caused by the elongation of the LGS due to the finite thickness of the sodium layer. In this paper, we model the LGS aberrations for the GMT's LTAO system. We find that the main aberration induced by the structure of the sodium layer is a focus term, which can be measured with a natural guide star and corrected. For subapertures with large numbers of pixels, other aberrations are negligible. However, if there are few pixels available, centroid errors resulting from pixelation and truncation of the spot lead to significant wavefront errors. Working with the assumption that the LGS aberrations affect all of the wavefront sensors in the same way, we propose a method that filters the LGS aberrations directly from the Shack-Hartmann centroids. This method is shown to be effective at removing the bulk of the LGS aberrations while having a small effect on the turbulence estimation.

1 Introduction

Laser guide stars (LGSs) are routinely used in existing telescopes to measure wavefront aberrations. Measurements made using LGSs are affected by the elongation of the image of the laser spot due to the finite thickness of the sodium layer. The elongation is proportional to the distance between the laser launch telescope and the subaperture of the Shack-Hartmann wavefront sensor (WFS) used to make the measurement. As a result of this elongation, there are errors in the centroid estimate. We use the name "LGS aberrations" to describe the difference between the measurements made with an elongated spot and what would be measured using a point source at the same altitude. Experience with the Keck II LGS AO system and analytical modeling have shown that using side-launched lasers can result in aberrations with a lot of power at low spatial frequencies.[1, 2] Those studies assume a single launch telescope is used to propagate all of the lasers. The Giant Magellan Telescope (GMT) is planning to use a laser tomography adaptive optics (LTAO) system with six LGSs in a regular hexagon. The baseline design calls for three launch telescopes at the edge of the primary mirror projecting two LGSs each, as shown in Figure 1. The alternative is to project all of the LGSs from behind the adaptive secondary mirror, but this is not desirable from an engineering standpoint. Several studies have found that there is a negligible difference in measurement noise error between side launch and center launch.[4–6] In LTAO systems, there is a small benefit to lauching from the side, while ground-layer adaptive optics (GLAO) systems have slightly better performance when launching from the center.

In this article, we investigate the magnitude of the LGS aberrations for the GMT with side-launched LGSs. The classical way to measure the LGS aberrations is to use a "truth" sensor guiding on a natural guide star (NGS).[1] The GMT's LTAO system will AO-correct the off-axis tip-tilt star using an additional dedicated DM. Unfortunately, it is not possible to derive the LGS aberrations from an AO-corrected off-axis NGS since the errors seen by the WFSs depends on the location of the launch telescope. This means that the measurements from each of the WFSs will be corrupted by different

[a] marcos@flatwavefronts.com

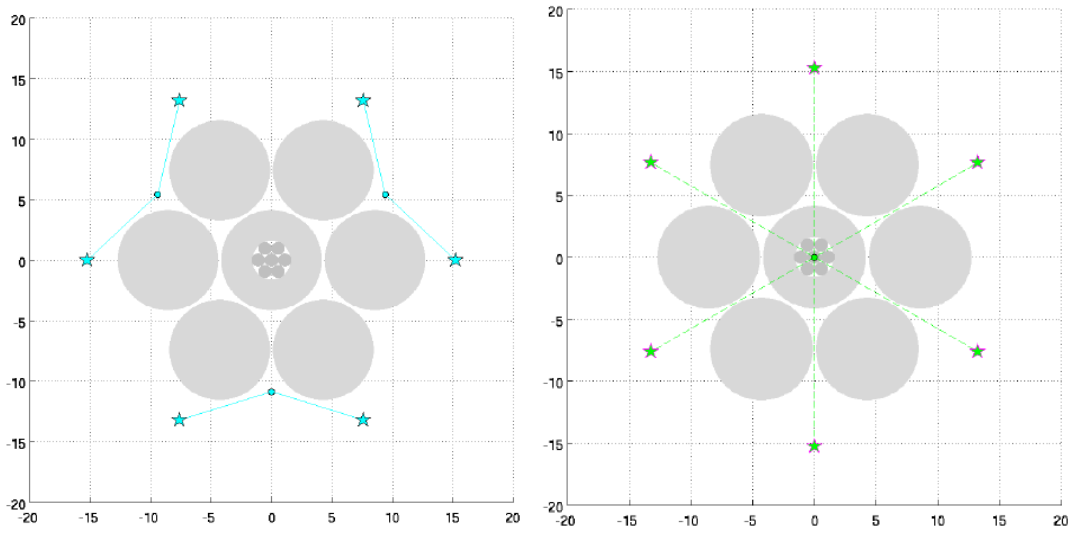

Fig. 1. Possible locations of the launch telescopes: side projection (left) or central projection (right).

centroid errors and the on-axis tomographic reconstruction of these centroid errors, seen by the science instrument, will differ from the off-axis reconstruction, seen by the truth sensor. In this report, we suggest an effective way to mitigate the effects of LGS aberrations by spatial filtering the centroids to remove patterns of centroids that are likely to be caused by LGS aberrations rather than atmospheric turbulence.

2 Sources of LGS aberrations

There are three known sources of LGS aberrations stemming from the vertical structure of the sodium layer: differential elongation, spot truncation and pixelation.

2.1 Differential elongation

To first order, the elongation η of the LGS is given by

$$\eta = \cos(\zeta) bt/h^2, \tag{1}$$

where ζ is the zenith angle, the baseline, b, is the distance between the subaperture and the laser launch telescope, and h and t are the height and thickness of the sodium layer. Even if the sodium layer structure is symmetrical, the lower part of the sodium layer will be more elongated than the upper part, leading to an asymmetrical spot. The elongation effect is proportional to h^{-2}. For a constant sodium profile, one would expect the intensity to vary as h^2: that is the intensity in the most elongated part of the spot (corresponding to lower altitude sodium) should be lower than the less elongated part of the spot (corresponding to higher altitude sodium). However, there is another effect that perfectly cancels out this variation in intensity. Due to the increased distance between the sodium atoms and the detector, the returned flux decreases with increasing height, with a h^{-2} dependency. As a result, the measured intensity distribution has exactly the same form as the structure in the sodium layer, except that there is a stretching in the coordinates: the structure at lower altitudes is stretched over a larger angle but without a corresponding reduction in intensity.

As an example, let us consider a sodium density profile that has a constant density between 85 km and 95 km above the telescope and zero elsewhere. The resulting image intensities when the sodium layer is imaged at baselines of 5, 10 and 20 m from the launch telescope are plotted in Figure 2.

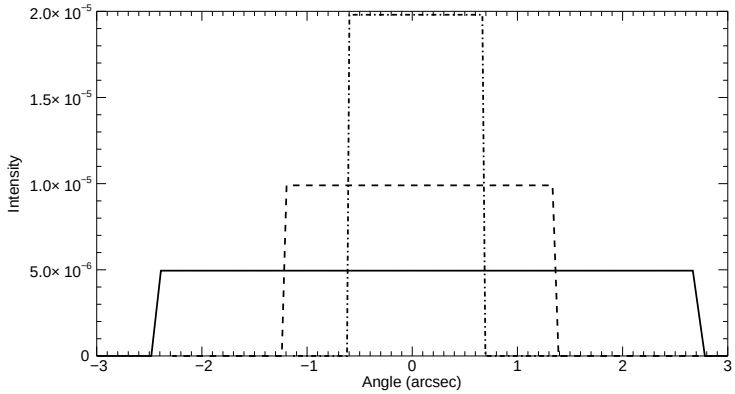

Fig. 2. Simulated spot elongation for a top-hat sodium layer distribution. The three intensity distributions correspond to baselines of 20 m (solid), 10 m (dashed) and 5 m (dot dashed). The reference angle corresponds to the return from the center of the sodium layer.

It can be seen that, while the resulting spots take the same form as the sodium density distribution, the elongation is stronger in one direction than the other, leading to a decentered image. The decentering is proportional to the baseline, so there is a linear increase in centroid error with distance between the launch telescope and the subaperture. When this centroid error is reconstructed, it leads to a focus error, which can be sensed with a natural guide star and removed. This focus error occurs for any abritrary sodium density distribution and is proportional to the square of the thickness of the turbulence layer. Note that the source of this focus error is different to that caused by fluctuations in the mean height of the sodium layer, but in practice they are indistinguishable.

In the remainder of the paper, we model the LGS aberrations by convolving the resulting spots with the expected seeing and intrinsic size of the laser beam. The resulting spots across the pupil can be seen in Figure 3.

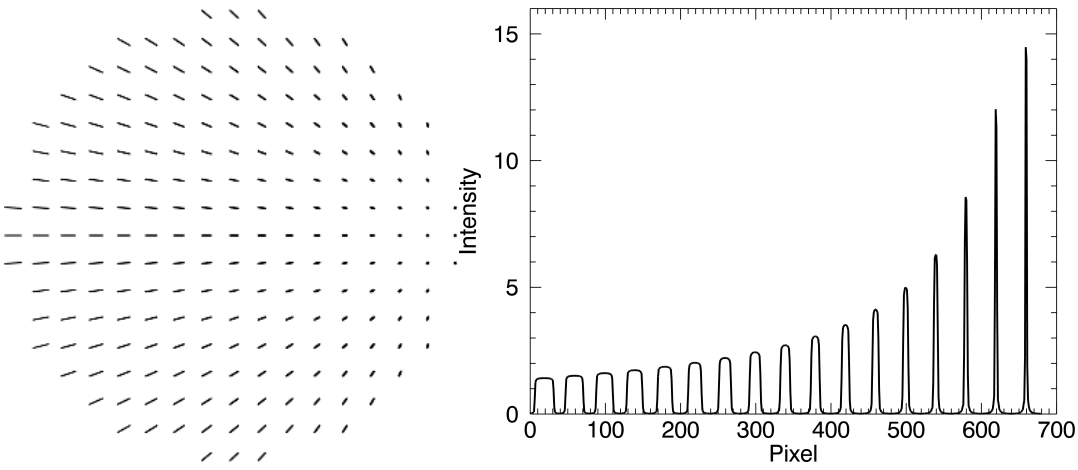

Fig. 3. Simulated spot elongation for a top-hat sodium layer (left) with a cross-section through the center (right).

2.2 Spot truncation

Spot truncation occurs when the size of the spot is larger than the detector extent, resulting in a bias in the centroid away. The magnitude of this error increases non-linearly with distance between the subaperture and the launch telescope. Its magnitude can be reduced by increasing the angular extent of the detector (more pixels or larger pixels) and by judicious choice of the centroiding algorithm. For example, the centroid estimate is very strongly affected since pixels far away from the center have a large weight, while a correlation algorithm would not suffer from this error if the intensity of the truncated component of the spot is known.

2.3 Pixelation

If the size of the pixel is large relative to the spot there will be a pixelation error, which ultimately constrains the maximum size of the pixels. The magnitude of this error increases with increasing structure in the vertical distribution of sodium atoms. An algorithm which uses knowledge of the spot profile and (explicitly or implicitly) interpolates the pixels will perform better.

3 Modeling the LGS aberrations

In this section, we investigate the magnitude of the LGS aberrations as a function of the number of pixels per subaperture. One thousand sodium density profiles were obtained from the University of British Columbia LIDAR study. The sodium density as a function of height was used to generate WFS spots in the following manner. First, the sodium density was binned into 35 different bins representing different altitudes between 80 and 100 km. Each of the bins was treated as an incoherent point source and used to generate an image at each subaperture. The image was convolved with a Gaussian with a FWHM of 1 arcsecond to take into account the seeing and the intrinsic size of the laser spot. The final image is the sum of the 35 different sources. The images are created at a high resolution and then rebinned according to the pixel size of the detector to create the WFS spots.

The spots were then centroided using the standard center-of-intensity algorithm and the centroid errors for each subaperture of each wavefront sensor were reported. Next, the tip-tilt and focus terms on each WFS were removed. This erases the effect of the differential spot elongation, which only produces tip-tilt and focus within each WFS. Finally, the centroids were tomographically reconstructed using the method of Ellerbroek[3] to give the on-axis LGS aberration. Figure 4 shows the reconstructed wavefront when using a 15×15 detector with 0.4” pixels.

The LGS aberrations, other than the focus error which has been removed, have a magnitude of 5 nm RMS. This is negligible. However, if the detector only has 4×4 pixels, such as is planned for the GMT’s GLAO system, the aberrations have an average wavefront of 40 nm RMS for the sodium profiles studied here. These errors are both acceptable. Nevertheless, we propose a technique to reduce the magnitude of the LGS aberrations.

4 Filtering the LGS aberrations

Here, we present a novel technique to reduce the effect of LGS aberrations, by filtering out centroid before reconstructing the wavefront.

We assume that the errors in the x- and y-centroid measurements, Δc_x and Δc_y, due to LGS aberrations measured by each of the six LGS wavefront sensors depend only on the distance between the launch telescope and the subaperture and take the form:

$$\Delta c_x = f(x_{SUBAP} - x_{LAUNCH}) \tag{2}$$

and

$$\Delta c_y = f(y_{SUBAP} - y_{LAUNCH}). \tag{3}$$

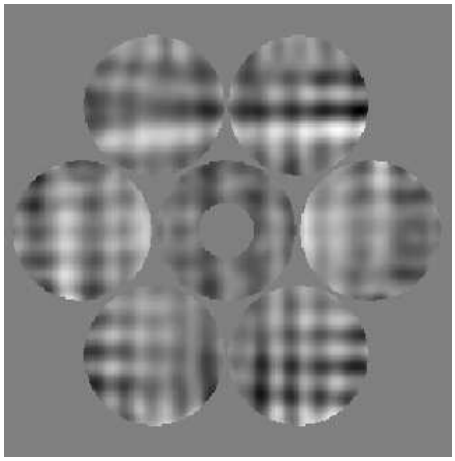

Fig. 4. LGS aberrations using 15x15, 0.4” pixels per subaperture. The RMS wavefront is 5 nm.

where x_{SUBAP} is the x-location of the subaperture and x_{LAUNCH} is the x-location of the launch telescope. The function f should be identical for both x and y axes and for all six wavefront sensors, although the location of the launch telescopes, (x_{LAUNCH}, y_{LAUNCH}), differs depending on the wavefront sensor. In this study, the launch telescopes are situated in an equilateral triangle as shown in Figure 1. The function f depends on static parameters, such as the number and size of pixels in the detector, and the algorithm used to determine the centroid, and on time varying parameters, such as the structure of the sodium layer, the zenith angle and the intrinsic size of the laser spot. The function $f(b)$, where b is the baseline between the centroid measurement and the laser, can be written as a low-order, odd polynomial:

$$f(b) \approx \alpha + k_1 b + k_3 b^3 + k_5 b^5 \ldots \tag{4}$$

The variable $\alpha = [\alpha_{\mathbf{x1}}, \alpha_{\mathbf{x1}}, \alpha_{\mathbf{x1}}, \alpha_{\mathbf{x1}}, \ldots]^{\mathbf{T}}$ represents the displacement of all the spots in a given WFS (i.e., the uncertainty in the location of the LGS) and is allowed to vary for each axis of each wavefront sensor, while the parameters of the function f, $\mathbf{k} = [k_1, k_2, k_3, \ldots]^T$ are forced to take the same value for all wavefront sensors and axes orientations. The parameter values are found using a least-squares fit of the centroid measurements, $\mathbf{c} = [c_{x1}, c_{y1}, c_{x2}, c_{y2}, \ldots]^T$, to the model. The fit consists of estimating the parameters α and $\mathbf{k}$ that minimize

$$\Sigma(\mathbf{c} - J\alpha - B\mathbf{k})^2 \tag{5}$$

where

$$J = \begin{bmatrix} 111\ldots & 000\ldots & 000\ldots\ldots \\ 000\ldots & 111\ldots & 000\ldots\ldots \\ \ldots & \ldots & \ldots \quad \ldots \end{bmatrix} \tag{6}$$

and

$$B = \begin{bmatrix} \mathbf{b} & \mathbf{b}^3 & \mathbf{b}^5 & \ldots \end{bmatrix} \tag{7}$$

Defining H = [J, B], we get the solution

$$\begin{bmatrix} \alpha \\ \mathbf{k} \end{bmatrix} = (H^T H)^{-1} H^T \mathbf{c}. \tag{8}$$

In practice, we first run a Gram-Schmidt orthogonalization on the columns of H before finding the pseudo-inverse.

It is now instructive to see what effect of each term in the expansion has on the reconstructed wavefront.

The constant terms, α, have no bearing on the wavefront reconstruction, because the mean x- and y-centroids are removed from the output of each wavefront sensor.

The linear term, $f(b) = k_1 b$, simply corresponds to a focus measurement: a focus in the wavefront, since the partial derivatives of a focus term, $g(x, y) = \frac{1}{2}(x^2 + y^2)$, are $\frac{\partial g(x,y)}{\partial x} = x$ and $\frac{\partial g(x,y)}{\partial y} = y$. All six wavefront sensors will see exactly the same focus error. When reconstructed tomographically, this leads to simply a focus term.

The higher-order terms reconstruct as more complicated 3D turbulence distributions that do not occur in the atmosphere.

The centroid error for the cases of 15x15 and 4x4 pixels per subaperture is plotted in Figure 5. It

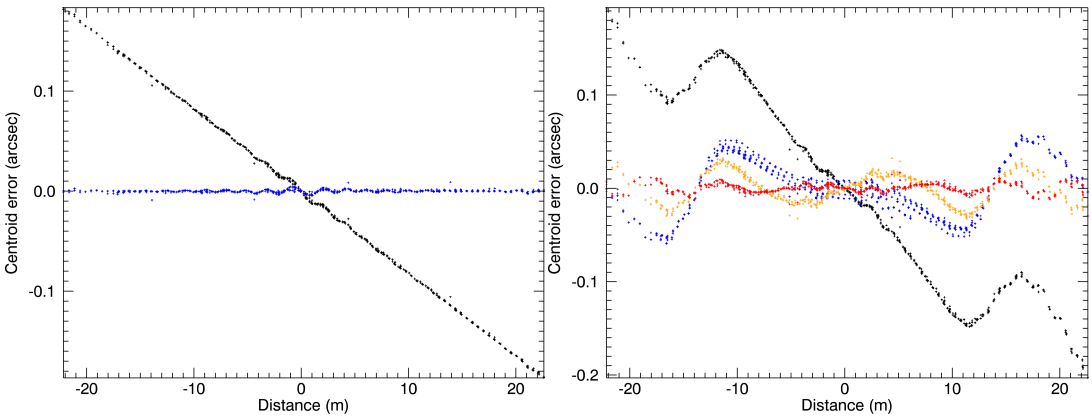

Fig. 5. Centroid error as a function of distance between the laser launch telescope and the subapertures for the case of 15x15 (left) and 4x4 (right) pixels per subaperture. The black line represents the raw centroid error. The blue, orange and red lines represent the centroid error after subtraction of the linear, fifth-order and ninth-order terms respectively.

shows that for the case of 15x15 pixels per subaperture, the only significant error in the centroids is the linear term, which when reconstructed corresponds to an error in focus. Fortunately, the focus error can easily be measured with an NGS and corrected. For the case of only 4x4 pixels per subaperture, there is a higher-order dependency of the centroid error on distance between the subaperture and the launch telescope. By removing up to the ninth-order, we can reduce the typical reconstructed LGS aberration from 40 nm to 5 nm RMS. The resulting on-axis wavefronts are displayed in Figure 6. It can be seen that most of the low spatial frequency structure has been removed from the wavefront.

End-to-end simulations were run using YAO to see what effect removing the higher-order terms has on turbulence compensation. In this case, the tip-tilt star was faint and 45 arcseconds away from the optical axis. The median atmospheric parameters for Las Campanas Observatories were used.[7] It was found that the K-band Strehl ratio dropped from 0.363 to 0.347 when removing up to the ninth-order. This shows that there is a modest penalty to be paid when filtering the LGS aberrations. In this case, the filtering would not be warranted. However, earlier modeling of the LGS aberrations incorrectly indicated that the magnitude of the LGS aberrations would be much larger.

5 Conclusion

This article investigates the magnitude and effect of LGS aberrations on side-launched LTAO systems for ELTs. It was found that changes in the structure in the sodium profile introduce an error in the focus measurement due to differential elongation of the LGS, which is of no consequence. Spot truncation and pixelation effects also introduce aberrations, but these aberrations are only significant if there are few pixels in the detector. For a typical sodium profile, the GMT will experience a tomographically reconstructed wavefront error of 5 nm and 40 nm RMS for the cases of 15x15 and 4x4 pixels per

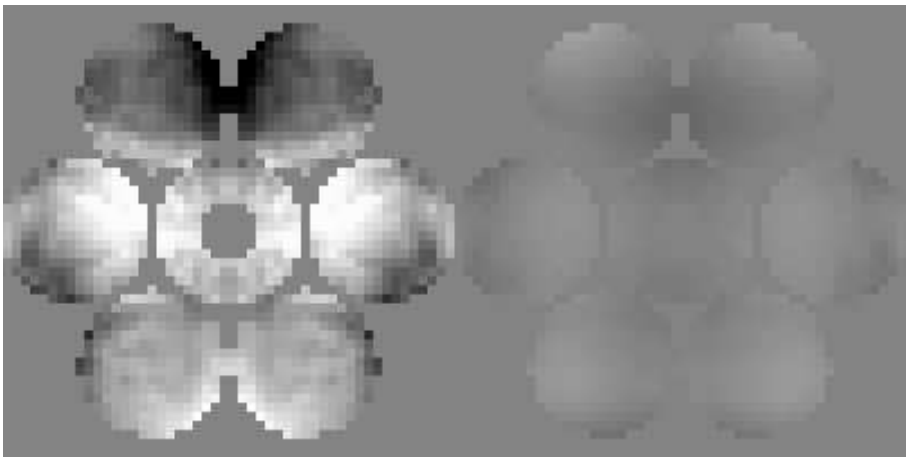

Fig. 6. LGS aberrations using 4x4 pixels before (left) and after (right) spatial filtering the centroids. The RMS wavefronts are 68 nm and 8 nm respectively.

subaperture. Finally, a spatial filtering method is presented that can be used to reduce the magnitude of the aberrations for the case where few pixels are available. This method relies on the fact that LGS aberrations depend only on the distance between the launch telescope and the subapertures.

References

1. M. A. van Dam et al, "Quasi-static aberrations induced by laser guide stars in adaptive optics," Optics Express 14, 7535-7540 (2006).
2. R. M. Clare et al, "Modeling low order aberrations in laser guide star adaptive optics systems," Opt Express 15 4711-4725 (2007).
3. B.L. Ellerbroek, "Efficient computation of minimum-variance wave-front reconstructors with sparse matrix techniques," J. Opt. Soc. Am. A 19, 1803-1816 (2002).
4. B. L. Ellerbroek, "TMT Laser guide star facility center launch versus side launch trade study report," TMT.AOS.TEC.10.018.REL02 (2010).
5. R. M. Clare and M. Le Louarn, "Simulations of Laser Guide Star Adaptive Optics Systems for the European Extremely Large Telescope," 1st AO4ELT conference, 03005 (2010).
6. C. Bechet et al, "Closed-loop ground layer adaptive optics simulations with elongated spots : impact of modeling noise correlations," 1st AO4ELT conference, 03004 (2010).
7. M. S. Goodwin, "Turbulence profiling at Siding Spring and Las Campanas Observatories," Ph.D. Thesis, Australian National University (2009).